Excitation Spectrum of Two Correlated Electrons in a Lateral Quantum Dot with Negligible Zeeman Splitting

C. Ellenberger,[1] T. Ihn,[1] C. Yannouleas,[2] U. Landman,[2] K. Ensslin,[1] D. Driscoll,[3] and A. C. Gossard[3]

[1]*Solid State Physics, ETH Zurich, 8093 Zurich, Switzerland*
[2]*School of Physics, Georgia Instititute of Technology, Atlanta, Georgia 30332-0430, USA*
[3]*Materials Department, University of California, Santa Barbara, California 93106, USA*

The excitation spectrum of a two-electron quantum dot is investigated by tunneling spectroscopy in conjunction with theoretical calculations. The dot made from a material with negligible Zeeman splitting has a moderate spatial anisotropy leading to a splitting of the two lowest triplet states at zero magnetic field. In addition to the well-known triplet excitation at zero magnetic field, two additional excited states are found at finite magnetic field. The lower one is identified as the second excited singlet state on the basis of an avoided crossing with the first excited singlet state at finite fields. The measured spectra are in remarkable agreement with exact-diagonalization calculations. The results prove the significance of electron correlations and suggest the formation of a state with Wigner-molecular properties at low magnetic fields.

Two-electron ($2e$) systems (e.g., the He atom [1] and the H_2 molecule [2]) have played an important role in the development of the theory of many-body effects in quantum mechanics and the understanding of the chemical bond. Recently, two-dimensional (2D) man-made quantum dots (QDs), fabricated in semiconductor materials, have attracted attention as a laboratory for investigations of few-body systems with highly controlled parameters [3–10] such as the electron number, confinement strength, inter-electron repulsion, and the influence of an applied magnetic field (B). Furthermore, $2e$ QDs may be used for implementing logic gates in quantum computing [11], or, as suggested recently [12], by using $2e$ singlet and triplet states as the two states of a qubit; here the $2e$ populate a single QD.

Earlier experiments on vertical QDs led to the observation of a singlet-triplet (ST) transition in the $2e$ ground state as a function of the magnetic field [4,5,7] and for $N \geq 2$ to an energy level shell structure reminiscent of the periodic table of natural atoms [6]. The spin-triplet excited state of the $2e$ system was investigated in Ref. [7] in finite bias tunneling experiments. Laterally defined few-electron dots [8] added investigations of the magnetic-field dependent ST gap for two electrons [9,10].

At low magnetic fields, the importance of electron correlations in 2D QDs (under appropriate conditions; see below), with different behavior compared to natural atoms, has been anticipated theoretically [13–19]. Clear experimental evidence for such strong correlation effects is still lacking (see, however, the very recent Ref. [10]). Insights can be gained through investigations of the excitation spectrum of $2e$ QDs in a perpendicular magnetic field. Here we report on joined experimental and theoretical endeavors that establish the correlated nature of the two electrons in our lateral QD, purposely fabricated to exhibit a negligible Zeeman splitting. We find that the explanation of the measured spectra requires a high level treatment of electron correlations in the dot, and cannot be accounted for by perturbative schemes starting from the independent-particle picture, or by spin-density functional theory (see footnote on p. 705 of Ref. [19]). The exact-diagonalization (EXD) calculations are in remarkable agreement with intricate measured features of the spectra, indicating the formation of an H_2-type Wigner molecule (WM) at low magnetic field, lifting of degeneracies, and the appearance of avoided crossings between excited singlet states associated with a shape anisotropy of our dot—as well as excitations resulting from relative and center-of-mass (c.m.) motion.

The sample is based on a 55 nm wide Ga[Al]As parabolic quantum well [20] with the center located 75 nm below the surface. The parabola ranges from 6% Al-concentration in the center to 23% at the edges. It was designed for having a g factor for electrons $|g| \approx 0$ following from the average material composition [21,22]. The effective mass of the electrons is higher than that of pure GaAs due to the larger band gap. We use the estimated value $m^* = 0.07m_0$, leading to an effective Rydberg energy $R_{Ry}^* = 6$ meV. The two-dimensional electron gas (2DEG) has a density $n_s = 4.5 \times 10^{15}$ m^{-2} and a mobility $\mu = 2.5$ m^2/V s at a temperature of 4.2 K. A highly Si-doped layer 1.76 μm below the surface acting as a backgate was not used during the experiments described below. The quantum dot (geometric diameter 220 nm) with integrated charge readout depicted in Fig. 1 (inset) was defined using electron beam lithography patterned split gates. All measurements were performed at an electronic temperature below 300 mK as estimated from the width of conductance resonances in the Coulomb-blockade regime.

Figure 1 shows the differential conductance of the QD in the plane of bias and plunger-gate voltages. It was measured by applying half of the dc bias voltage, $V_{bias}/2$, to the source and $-V_{bias}/2$ to the drain contact. The recorded
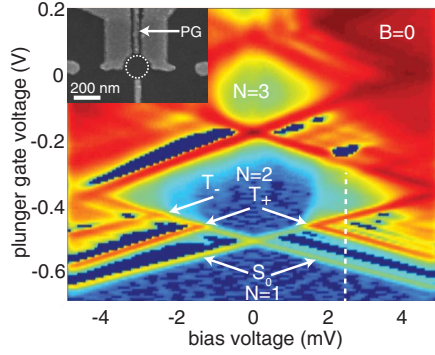
FIG. 1 (color online). Differential conductance dI/dV_{bias} at zero magnetic field. Electron numbers N are indicated in the diamonds. The arrows mark the transitions between the one-electron ground state and the $2e$ spin-singlet (S_0) and spin-triplet states (T). Inset: scanning electron micrograph of the sample. The quantum dot is marked with a dotted circle and PG labels the plunger gate. The vertical dashed line marks the bias voltage for which the data in Fig. 2 is taken.

current I was numerically differentiated in order to obtain the differential conductance dI/dV_{bias}. The resulting diamond pattern of suppressed conductance corresponds to fixed electron numbers N in the dot as indicated in the figure.

The values for the electron numbers were found by depleting the dot down to zero electrons with more negative gate voltages (not shown) and by using the quantum point contact near the quantum dot as a charge detector. For these modified gate voltage settings we observed the first single-particle excited state of the $N = 1$ quantum dot at an energy $\Delta_1 = 5$ meV above the ground state and found an addition energy $\Delta\mu_2 = 6.9$ meV (both Δ_1 and $\Delta\mu_2$ are outside the range shown in Fig. 1). These numbers show that in this dot, confinement effects (Δ_1) and interaction effects ($\Delta\mu_2$) are comparable in magnitude. Furthermore, the electronic size estimated via $\sqrt{\hbar^2/m\Delta_1}$ is much smaller than the electronic mean free path.

Returning to Fig. 1, we determine from the extent of the $N = 2$ diamond in bias direction the addition energy $\Delta\mu_3 = 5.1$ meV for adding the third electron to the dot. The strong lines labeled S_0 in the figure correspond to tunneling transitions between the one-electron ground state and the $2e$ spin-singlet ground state.

Strong lines parallel to the diamond boundaries outside the diamonds correspond to excited states of the level spectrum. In Fig. 1, we see the transition T_+ between the one-electron ground state and the first excited $2e$ triplet state. The energy separation between the singlet and this triplet state is $J = 1.7$ meV. For negative bias voltage we see an additional excited state T_- which we attribute to the second triplet state split from T_+ by 1.5 meV due to the deviation of the dot potential from circular shape (see also Fig. 4 below). Negative differential conductance can arise due to asymmetric coupling of states to source and drain. Inside the diamonds, higher order (cotunneling) processes can be seen for $N \geq 2$ [23].

In order to investigate the evolution of the excited state spectrum with magnetic field, we have measured the current at fixed $V_{\text{bias}} = 2.5$ mV. In Fig. 2 we plot the derivative dI/dV_{pg}. Resonances in dI/dV_{pg} correspond to resonances in the differential conductance dI/dV_{bias}. The resonances indicated by symbols in the plot are labeled consistently with Fig. 1. It can be seen that the ST separation $J(B) = E_{T_+} - E_{S_0}$ between the S_0 and the T_+ states decreases with magnetic field and becomes zero at $B_{\text{ST}} \approx 4$ T. Beyond this field, the energy of the S_0 state continues to increase and exhibits an avoided crossing with another excited state S_2 which appears above 2.7 T. The avoided crossing suggests that S_2 is an excited spin-singlet state and that the deviation of the dot potential from axial symmetry causes level repulsion. A third excited state ($T_{+,\text{c.m.}}$) appears at even higher plunger-gate voltage. This state is shown below (see Fig. 4) to be a triplet excited state associated with the c.m. motion of the $2e$ molecule.

A qualitative indication of the importance of correlation effects can be obtained via the Wigner parameter $R_W = (e^2/\kappa l_0)/\hbar\omega_0$, i.e., the ratio of the Coulomb interaction for two electrons at distance $l_0 = \sqrt{\hbar/m^\star\omega_0}$ and the single-particle level spacing in a circular harmonic confinement, $\hbar\omega_0$ [15]. Correlation effects are of increasing importance when the interaction energy becomes dominant over the single-particle spacing, i.e., when $R_W > 1$. Using a conservative estimate for the confinement energy of 5 meV (as quoted above for the dot with zero or one electrons), we find $R_W \approx 1.55$ indicating that correlations may indeed have a certain significance.

Quantitative understanding of the measured excitation spectrum and of the underlying strong correlations in the $2e$ QD were obtained through exact diagonalization of the Hamiltonian for two 2D interacting electrons

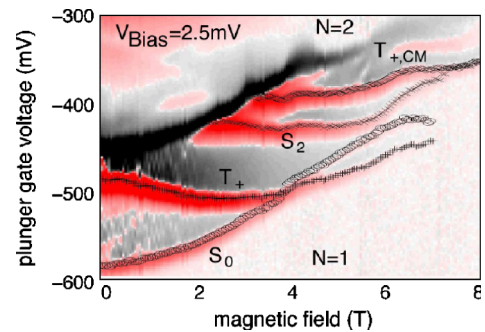$$\mathcal{H} = H(\mathbf{r}_1) + H(\mathbf{r}_2) + \gamma e^2/(\kappa r_{12}), \quad (1)$$

FIG. 2 (color online). Differentiated current dI/dV_{pg} at $V_{\text{bias}} = 2.5$ mV. Gray striped regions (red online) marked by symbols correspond to positive (peaks) dI/dV_{pg}. The dark black region (also black online) corresponds to negative dI/dV_{pg}. Electron numbers N are indicated. Transitions between the one-electron ground state and the $2e$ spin-singlet ground state (S_0), spin-triplet excited state (T_+) and spin-singlet excited state (S_2) are labeled.

where the last term is the Coulomb repulsion, κ (12.5 for GaAs) is the dielectric constant, and $r_{12} = |\mathbf{r}_1 - \mathbf{r}_2|$. The prefactor γ accounts for the reduction of the Coulomb strength due to the finite thickness of the electron layer in the z direction and for any additional screening effects due to the gate electrons. $H(\mathbf{r})$ is the single-particle Hamiltonian, which for an anisotropic, harmonically confined QD, is written as

$$H(\mathbf{r}) = T + \frac{1}{2}m^*(\omega_x^2 x^2 + \omega_y^2 y^2), \qquad (2)$$

where $T = (\mathbf{p} - e\mathbf{A}/c)^2/2m^*$, with $\mathbf{A} = 0.5(-By, Bx, 0)$ being the vector potential in the symmetric gauge. The effective mass is $m^* = 0.07m_0$, and $\mathbf{p}$ is the linear momentum of the electron. The second term is the external confining potential. In the Hamiltonian (2), we neglect the Zeeman contribution due to the negligible value ($g^* \approx 0$) of the effective Landé factor in our sample.

In the EXD method, the many-body wave function is written as a linear superposition over the basis of noninteracting $2e$ determinants, i.e.,

$$\Psi_{\mathrm{EXD}}^{s,t}(\mathbf{r}_1, \mathbf{r}_2) = \sum_{i<j}^{2K} \Omega_{ij}^{s,t}|\psi(1;i)\psi(2;j)\rangle, \qquad (3)$$

where $\psi(1;i) = \varphi_i(\mathbf{r}_1)\alpha(1)$ if $1 \leq i \leq K$ and $\psi(1;i) = \varphi_{i-K}(\mathbf{r}_1)\beta(1)$ if $K+1 \leq i \leq 2K$ [and similarly for $\psi(2,j)$], with $\alpha(\beta)$ denoting up (down) spins; the index i (or j) $\equiv (k, l)$ and $\varphi_i(\mathbf{r}) = X_k(x)Y_l(y)$, with $X_k(Y_l)$ being the eigenfunctions of the one-dimensional oscillator in the x (y) direction with frequency ω_x (ω_y). In the calculations we use $K = 79$, yielding convergent results. The total energies $E_{\mathrm{EXD}}^{s,t}$ and the coefficients $\Omega_{ij}^{s,t}$ are obtained through a "brute force" diagonalization of the matrix eigenvalue equation corresponding to the Hamiltonian in Eq. (1).

Figure 3 shows the experimentally extracted energy splitting $J(B)$ between the states S_0 and T_+ together with results of the EXD calculations with $\hbar\omega_x = 4.23$ meV, $\hbar\omega_y = 5.84$ meV [i.e., $\hbar\omega_0 = \hbar\sqrt{(\omega_x^2 + \omega_y^2)/2} = 5.1$ meV], and $\gamma = 0.862$. With this value of γ, the Wigner parameter $R_W = 1.34$. The anisotropy used in the calculations is $\omega_y/\omega_x = 1.38$ indicating that the quantum dot considered here is closer to being circular than in other experimental systems [9,10].

To assess the dot parameters determined from the comparison between the measured and calculated $J(B)$, we checked that varying the value of ω_0 (while keeping $\omega_y/\omega_x = 1.38$) and the parameter γ does not influence substantially the quality of the fit to the experimental $J(B)$—as long as $\hbar\omega_0$ does not deviate greatly (i.e., more than 20%) from the $N = 1$ single-particle excitation Δ_1. Such a range of variations in the dot parameters is reasonable for the given sample and its measured $N = 1$ excitation and charging energies and is due to changes in the confinement with changing V_{pg}.
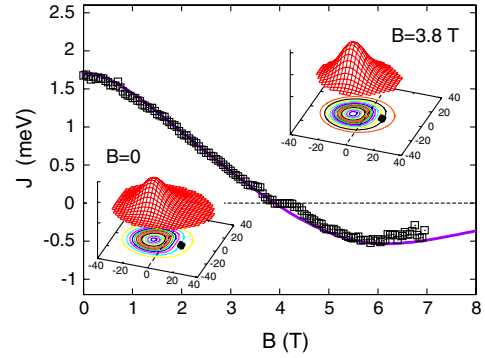

FIG. 3 (color online). The ST splitting $J(B)$ extracted from the experiment (open squares) together with the calculated EXD results (solid line). For the dot parameters, see text. Inset: Conditional probability distributions for the second electron when the first is held fixed at the point indicated by the solid dot. For the $2e$ QD that we studied, the Wigner molecule character is gradually enhanced with increasing magnetic field. Lengths are in nm, and CPDs in arbitrary units.

The inset of Fig. 3 shows the EXD calculated singlet conditional probability distributions (CPDs) [17,18,24,25] for the second electron, given that the first electron is kept fixed at a given location (indicated by a solid dot). The electrons clearly tend to avoid each other reflecting their strongly correlated motion, in contrast to the two electrons in the natural Helium atom that occupy the same single-particle orbital. Comparison of the CPDs for $B = 0$ and $B = 3.8$ T shows that the magnetic field leads to an enhancement of the correlation between the two electrons resulting in a sharpening of the Wigner-molecular state. Larger values of B result in an effective dissociation [19] of the WM in analogy to the dissociation of the natural H_2 [2], leading eventually to a vanishing of $J(B)$, in agreement with the trend seen in Fig. 2. We emphasize that the negligible Zeeman splitting in our sample is crucial for the observation of this trend which should even lead to ST oscillations of the ground state spins at higher magnetic fields [13]. Experimentally, however, the accessible magnetic-field range is limited, because conductance resonances disappear with increasing field due to wave function shrinkage, and counterbalancing this effect by changing gate voltages would seriously change the confinement potential.

The EXD calculated spectrum of the elliptic $2e$ QD is displayed in Fig. 4. The thick curves (colored online) correspond to features highlighted in the experimental spectrum (see Fig. 2) in the region between $N = 1$ and $N = 2$. The good overall agreement between the measured and calculated spectra allows for a full interpretation of the observed features and their physical origins rooted in strong electronic correlations. The energy difference between the T_+ and S_0 states and its variation with B were discussed above [see $J(B)$ in Fig. 3].

Further interpretation is facilitated by consideration of the EXD calculated spectrum of the corresponding circular
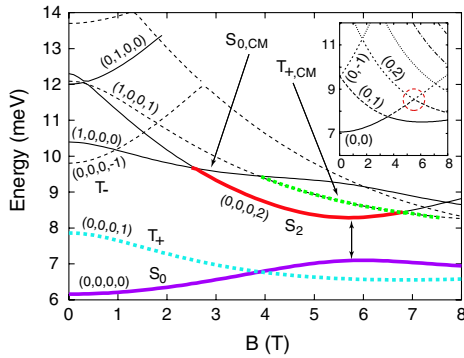
FIG. 4 (color online).   Calculated EXD energy spectrum, referenced to $2\hbar\sqrt{\omega_0^2 + \omega_c^2/4}$, in a magnetic field of a $2e$ dot with anisotropic harmonic confinement (for the dot parameters, see text). We have adopted the notation (N_x, N_y, n, m), where (N_x, N_y) refer to the c.m. motion along the x and y axes and (n, m) refer to the number of radial nodes and angular momentum of the relative motion in the corresponding *circular* dot. Inset: The EXD spectrum of the corresponding circular dot. Only the (n, m) indices are shown, since $N_x = N_y = 0$ for all the plotted curves. Solid lines denote singlets. Dashed lines denote triplets.

dot (Fig. 4, inset) where all the many-body energy levels $(0, m)$ with zero nodes and angular momentum index $m > 0$ decrease in energy with increasing magnetic field, converging at much higher B to the lowest Landau level of the interacting electrons. Since the deformation of the elliptic QD discussed here is moderate, we adopt in Fig. 4 the same notation as for the circular dot (see caption of Fig. 4). The second excited singlet state seen in the experiment (Fig. 2) and its avoided crossing with the first excited singlet state at $B \approx 5.8$ T is well reproduced by the theory [see curves marked as S_2 (red online) and S_0 (magenta online) in Fig. 4; the avoided crossing is marked by a double arrow] [26]. The third excited state, $T_{+,\text{c.m.}}$, is identified as a $(1,0,0,1)$ triplet excited state (green online) that is related to the T_+ state (blue online) through a c.m. excitation along the x direction. We note here that the aforementioned avoided crossing between the S_0 and the S_2 excited states developed as a result of the shape deformation of the dot and out of the crossing between the $(0,0)$ and $(0,2)$ singlets of the circular dot (marked by a circle in the inset). Another correspondence between the measured and calculated spectra is the splitting at $B = 0$ between the T_+ and T_- states (measured as 1.5 meV and calculated to be 1.9 meV); these triplet states are degenerate for the circular dot (see inset).

In conclusion, we have presented measurements of the excitation spectra of a lateral $2e$ QD—with negligible Zeeman splitting, moderate anisotropy, and parabolic z confinement being the main differences to systems investigated earlier. Exact-diagonalization calculations, including a rather small (14%) decrease in the effective interelectron Coulomb repulsion, explain in detail the ob-

served features of the spectra under the influence of a variable magnetic field, including the variation of the ST splitting, J. Theoretical analysis of the salient excitation-spectra patterns (e.g., avoided level crossings, the line shape of $J(B)$, and the lifting of level degeneracies in comparison to the circular case) indicates significant electronic correlations associated with formation of a Wigner molecule. The behavior of $J(B)$ for larger fields suggests an analogy between the dissociation process of the WM and that of the natural H_2 molecule. These results will assist the design of quantum-dot based devices and our understanding of other recent measurements on few-electron quantum dots [7,9,10].

[1] G. Tanner *et al.*, Rev. Mod. Phys. **72,** 497 (2000).
[2] W. Kolos and L. Wolniewicz, J. Chem. Phys. **49,** 404 (1968).
[3] B. Meurer *et al.*, Phys. Rev. Lett. **68,** 1371 (1992).
[4] R. C. Ashoori *et al.*, Phys. Rev. Lett. **71,** 613 (1993).
[5] T. Schmidt *et al.*, Phys. Rev. B **51,** R5570 (1995).
[6] S. Tarucha *et al.*, Phys. Rev. Lett. **77,** 3613 (1996).
[7] L. P. Kouwenhoven *et al.*, Science **278,** 1788 (1997); W. G. van der Wiel *et al.*, Physica (Amsterdam) **256–258B,** 173 (1998).
[8] M. Ciorga *et al.*, Phys. Rev. B **61,** R16315 (2000).
[9] J. Kyriakidis *et al.*, Phys. Rev. B **66,** 035320 (2002).
[10] D. M. Zumbühl *et al.*, Phys. Rev. Lett. **93,** 256801 (2004); C. Yannouleas and U. Landman, Proc. Natl. Acad. Sci. U.S.A. (to be published).
[11] D. Loss and D. P. DiVincenzo, Phys. Rev. A **57,** 120 (1998).
[12] J. M. Taylor *et al.*, Nature Phys. **1,** 177 (2005).
[13] M. Wagner *et al.*, Phys. Rev. B **45,** R1951 (1992).
[14] D. Pfannkuche *et al.*, Phys. Rev. B **47,** 2244 (1993).
[15] C. Yannouleas and U. Landman, Phys. Rev. Lett. **82,** 5325 (1999).
[16] R. Egger *et al.*, Phys. Rev. Lett. **82,** 3320 (1999).
[17] C. Yannouleas and U. Landman, Phys. Rev. Lett. **85,** 1726 (2000).
[18] S. A. Mikhailov, Phys. Rev. B **65,** 115312 (2002).
[19] C. Yannouleas and U. Landman, Int. J. Quantum Chem. **90,** 699 (2002).
[20] M. Sundaram *et al.*, Superlattices Microstruct. **4,** 683 (1988).
[21] C. Weisbuch and C. Hermann, Phys. Rev. B **15,** 816 (1977).
[22] G. Salis *et al.*, Nature (London) **414,** 619 (2001).
[23] S. De Franceschi *et al.*, Phys. Rev. Lett. **86,** 878 (2001).
[24] P. A. Maksym, Phys. Rev. B **53,** 10 871 (1996).
[25] C. Yannouleas and U. Landman, Phys. Rev. B **70,** 235319 (2004).
[26] The larger calculated energy gap at the avoided crossing in comparison to the measured value may be due to deviations from a harmonic confinement.